

Charge-magnetic roughness correlations in an Fe/Gd multilayer

C. S. Nelson

*Advanced Photon Source, Argonne National Laboratory, Argonne, Illinois 60439
and Department of Physics and Astronomy, Northwestern University, Evanston, Illinois 60208*

G. Srajer, J. C. Lang, C. T. Venkataraman, and S. K. Sinha

Advanced Photon Source, Argonne National Laboratory, Argonne, Illinois 60439

H. Hashizume and N. Ishimatsu

Materials and Structure Laboratory, Tokyo Institute of Technology, Nagatsuta, Midori, Yokohama 226-8503, Japan

N. Hosoito

Institute for Chemical Research, Kyoto University, Uji 611-0011, Japan

(Received 18 March 1999; revised manuscript received 4 August 1999)

Charge-magnetic roughness correlations of the Gd layers in an Fe/Gd multilayer are studied using diffuse, x-ray resonant magnetic scattering. The strong interfacial coupling exhibited by this system, which restricts the orientation of the magnetic moments, makes possible a detailed study of the intrinsic charge-magnetic roughness. Quantitative analysis of the data is carried out by using a newly developed model, based on the Born approximation, for diffuse, x-ray resonant magnetic scattering from multilayers. Fits to the charge and charge-magnetic interference data result in longer correlation lengths for both in-plane and out-of-plane charge-magnetic roughness than for charge roughness. [S0163-1829(99)10241-8]

I. INTRODUCTION

Interface structure plays a role in many of the interesting phenomena exhibited by magnetic films and multilayers, such as magnetization reversal processes, magnetic anisotropy, and exchange coupling of magnetic films through non-magnetic films. The characterization of interface parameters is therefore an important step in modeling the behavior of magnetic films and multilayers. Unfortunately, conventional x-ray techniques used to study interface structure, such as reflectivity and diffuse scattering, are sensitive only to the electron density, or charge, information. For a complete understanding of interface structure, a technique sensitive to the magnetic information is a necessity. Such a technique is x-ray resonant magnetic scattering (XRMS), which has been used to date to study transition-metal films.^{1,2} These studies report both a smaller rms magnetic roughness than rms charge roughness and a longer in-plane correlation length for charge-magnetic roughness than for charge roughness. Both of these features are thought to be due to the weak coupling of interface magnetic moments to the “bulk” magnetization of the film. Therefore, the differences in the roughness parameters are merely a selection effect due to the dependence of the magnetic scattering on the direction of the magnetic moments. In this paper, we take a closer look at the intrinsic charge-magnetic roughness by eliminating this possible explanation for the differences between the charge and magnetic roughness parameters. This is accomplished by studying a system with strong interfacial coupling—an Fe/Gd multilayer—and comparing the charge and charge-magnetic roughness correlation lengths. The use of this system provides an additional advantage due to its rare-earth component, which has resonances in the hard x-ray regime.

The increased penetration provided by the use of hard x rays makes possible the study of out-of-plane—in addition to in-plane—roughness correlations.

The second objective of this paper is to report the development of a model for the diffuse XRMS. This model is based on the Born approximation (BA) in which a perturbation of charge and magnetic roughness is used to calculate the diffuse XRMS from a multilayer. The quantitative results presented in this paper are obtained through fits to the data using this model. Finally, we will show and discuss anomalous scattering features and interference effects between the different charge and magnetic structures of the multilayer.

II. EXPERIMENT AND DATA

Diffuse XRMS data were collected on beamline 1-ID of the SRI CAT at the Advanced Photon Source, using the setup shown in Fig. 1. A double-crystal Si(111) monochromator was used to select an energy ≈ 2 eV above the Gd L_3 edge (7.243 keV). This energy was chosen because it corresponds to the maximum in the circular magnetic x-ray dichroism spectrum. The predominantly linearly polarized beam was converted to $>99\%$ circularly polarized beam by a diamond (111) phase retarder. The rotation of the phase retarder was carried out through the use of a piezoelectric transducer (PZT) and lever arm, which allowed for rapid helicity reversal of the x-ray beam. Finally, after reflection from a harmonic rejection mirror, the beam was incident on a vacuum-deposited Fe/Gd multilayer, which was placed between the poles of a permanent magnet with the field (≈ 3.4 kG) applied parallel to the surface of the multilayer.

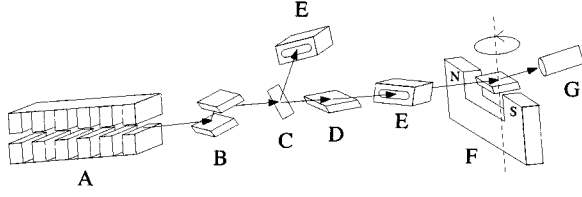


FIG. 1. Experimental setup on beamline 1-ID. Components include the undulator (A); double-crystal Si(111) monochromator (B); diamond phase retarder (C); harmonic rejection mirror (D); ionization chambers (E); permanent magnet and sample (F), which can be rotated about the surface normal of the sample; and Si(Li) solid-state detector (G).

The structural parameters of the multilayer were determined by measuring the specular reflectivity with circularly polarized x rays. The sum of the reflectivity measured with opposite photon helicities was used to determine the structural parameters through a modified—Parratt fit³ (see Fig. 2). The nominal Si cap/[Fe(35 Å)/Gd(52 Å)]₁₅/Si substrate structure was modeled as Si/Fe silicide/Fe/[Gd/Fe]₁₄/Gd/Si substrate due to the expected formation of iron silicide at the interface between the silicon cap and the first iron layer.⁴ The fitted structure was determined to be Si(19.9 Å)/Fe silicide(19.5 Å)/Fe(36.1 Å)/[Gd(53.2 Å)/Fe(36.4 Å)]₁₄/Gd(53.2 Å)/Si substrate. Note that for all fits described in this paper, Fe/Gd and Gd/Fe interfaces were treated as identical.

At room temperature, the spin structure of the multilayer is expected to be in an aligned state, with all of the Fe (Gd) magnetic moments parallel (antiparallel) to the applied field.⁵ This was verified by taking advantage of the geometrical dependence of the XRMS, which requires the magnetic moments to be in the scattering plane (see Sec. III). By subtracting the reflectivity measured with opposite photon helicities and with the applied field parallel and then perpendicular to the scattering plane, these measurements showed that the multilayer was in an aligned state, with no component of the Gd magnetic moment perpendicular to the applied field. All

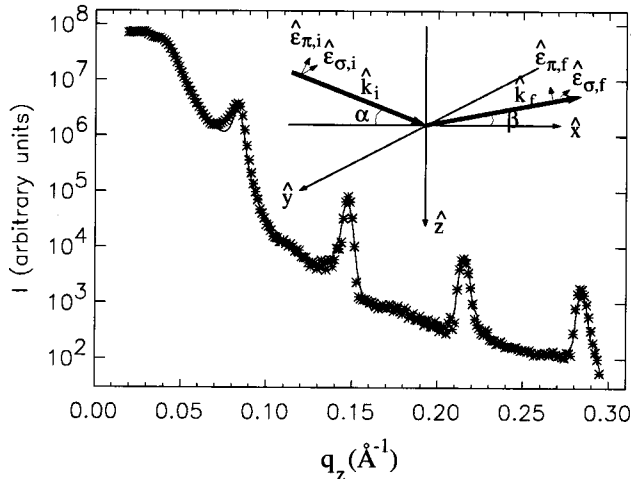


FIG. 2. Specular reflectivity (*) with modified Parratt fit (-). Statistical error bars are smaller than the size of the symbol. Inset shows the scattering geometry.

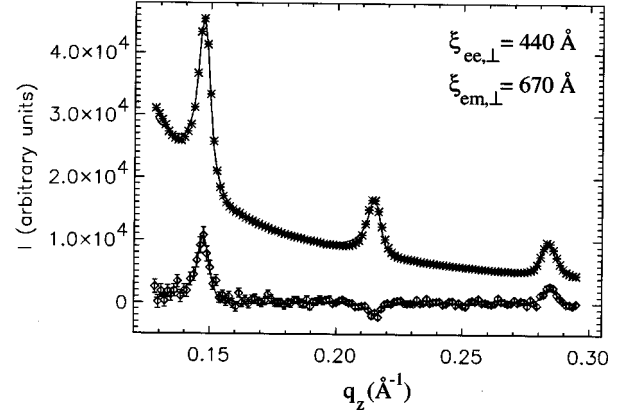


FIG. 3. Sum (*) and difference (◇) of opposite helicity offset scans, with BA fits (-). Statistical error bars for the summed data are smaller than the size of the symbol.

subsequent measurements were made with the applied field parallel to the scattering plane.

The diffuse XRMS data collected consist of an offset scan, mostly along q_z (see inset in Fig. 2 for the scattering geometry), in which the detector angle was offset from the specular peak by 0.24° , and two rocking curves taken at $q_z \approx 0.147 \text{ \AA}^{-1}$ and 0.215 \AA^{-1} (over the second and third multilayer Bragg peaks). Charge diffuse and diffuse XRMS data were extracted from these three scans by taking the sum and difference, respectively, of the data from opposite photon helicities.

The sum and difference offset scans, shown in Fig. 3, exhibit peaks at q_z corresponding to the multilayer Bragg peaks, which are due to out-of-plane correlations in the interface roughness. Another obvious feature in Fig. 3 is the sign reversal of adjacent peaks in the difference data, which has also been seen in specular XRMS data.^{6,7} This is caused by a nonuniform magnetic moment distribution within the Gd layers, which is to be expected as the strong coupling of the Fe and Gd atoms at the interfaces allows the interfacial Gd atoms to remain ferromagnetic above the bulk Gd Curie temperature.⁸ The change in sign of the charge-magnetic scattering as a function of q_z is therefore the result of an interference effect between the different charge and magnetic structures of the multilayer.

III. BORN APPROXIMATION MODEL OF DIFFUSE XRMS

In order to fit the diffuse XRMS data and make a quantitative comparison with the charge diffuse scattering, a theoretical model of the diffuse scattering difference signal in a multilayer is required. While following the approach of Osgood *et al.*,⁹ we begin to develop such a model with the expression for the elastic scattering amplitude for a single resonant ion using the electric dipole approximation. To leading order, this amplitude is¹⁰

$$f = -Zr_0 \hat{\epsilon}_f^* \cdot \hat{\epsilon}_i + \frac{3\lambda}{8\pi} \{ [F_1^+ + F_{-1}^-] \hat{\epsilon}_f^* \cdot \hat{\epsilon}_i + i [F_{-1}^+ - F_1^-] \times (\hat{\epsilon}_f^* \times \hat{\epsilon}_i) \cdot \hat{m} + [2F_0^+ - F_1^- - F_{-1}^-] (\hat{\epsilon}_f^* \cdot \hat{m})(\hat{\epsilon}_i \cdot \hat{m}) \}, \quad (1)$$

where $-Zr_0$ is the Thomson scattering amplitude per ion, the $\hat{\epsilon}$'s are initial and final photon polarizations, the F_M^L 's are dipole transition matrix elements, and \hat{m} is the ion's magnetic moment direction. The much smaller, nonresonant magnetic scattering is not included in the amplitude.

The first approximation in this treatment is that $[F_{-1}^1 - F_1^1] \gg [2F_0^1 - F_1^1 - F_{-1}^1]$. This is generally satisfied for rare-earth L edges,¹¹ and so we ignore the last term in Eq. (1). The next step is to extend the scattering amplitude to a system of scatterers, such as a layer of identical ions, and perturb the surfaces of the scattering system with both charge and magnetic roughness. Using the BA, the differential cross section is then written

$$\begin{aligned} \frac{d\sigma}{d\Omega} = & \left\{ N_e(-Zr_0) + N_r \frac{3\lambda}{8\pi} [F_1^1 + F_{-1}^1] \right\} \hat{\epsilon}_f^* \cdot \hat{\epsilon}_i \\ & \times \int \int \int_{V_e} e^{-i\mathbf{q} \cdot \mathbf{r}} d^3r + iN_r \frac{3\lambda}{8\pi} [F_{-1}^1 - F_1^1] \\ & \times (\hat{\epsilon}_f^* \times \hat{\epsilon}_i) \cdot \hat{m} \int \int \int_{V_m} e^{-i\mathbf{q} \cdot \mathbf{r}} d^3r \Big|^2, \end{aligned} \quad (2)$$

where N_e and N_r are the number densities of all electrons and the resonant electrons, respectively, and the integrals are over the total charge volume (V_e) and the magnetic, resonant orbital volume (V_m).

When multiplied out, Eq. (2) can be grouped into three terms—a pure charge term, a pure magnetic term, and an imaginary, interference term. The only term that is sensitive to the reversal of the photon helicity, however, is the interference term:

$$\begin{aligned} \left(\frac{d\sigma}{d\Omega} \right)_{\text{int}} = & \left[\left\{ N_e(-Zr_0) + N_r \frac{3\lambda}{8\pi} [F_1^1 + F_{-1}^1] \right\} \right. \\ & \times (\hat{\epsilon}_f^* \cdot \hat{\epsilon}_i)^* iN_r \frac{3\lambda}{8\pi} [F_{-1}^1 - F_1^1] [(\hat{\epsilon}_f^* \times \hat{\epsilon}_i) \cdot \hat{m}] \\ & \left. + \text{c.c.} \right] \int \int \int_{V_e} \int \int \int_{V_m} e^{-i\mathbf{q} \cdot (\mathbf{r}-\mathbf{r}')} d^3r d^3r', \end{aligned} \quad (3)$$

where c.c. is the complex conjugate of the previous term.

To calculate the polarization dependence, the degree of circular polarization is alternately reversed between a value of $+P_c$ and $-P_c$, which results in the following for the difference signal, differential cross section between positive and negative helicity:

$$\begin{aligned} \Delta \left(\frac{d\sigma}{d\Omega} \right) = & P_c [\hat{k}_f \cdot \hat{m} + \cos(\alpha + \beta) \hat{k}_i \cdot \hat{m}] \left[\left\{ N_e(-Zr_0) \right. \right. \\ & \left. \left. + N_r \frac{3\lambda}{8\pi} [F_1^1 + F_{-1}^1]^* \right\} N_r \frac{3\lambda}{8\pi} [F_{-1}^1 - F_1^1] + \text{c.c.} \right] \\ & \times \int \int \int_{V_e} \int \int \int_{V_m} e^{-i\mathbf{q} \cdot (\mathbf{r}-\mathbf{r}')} d^3r d^3r'. \end{aligned} \quad (4)$$

To evaluate the integrals, the approach of Sinha *et al.*¹² is followed. A Gaussian distribution of $z_e(x, y) - z_m(x', y')$ is assumed, and defining $\langle z_e^2 \rangle \equiv \sigma_e^2$ (mean-squared charge roughness), $\langle z_m^2 \rangle \equiv \sigma_m^2$ (mean-squared magnetic roughness), and $\langle z_e z_m \rangle \equiv C_{em}(X, Y)$ (charge-magnetic correlation function), the double integral is:

$$\begin{aligned} & \int \int \int_{V_e} \int \int \int_{V_m} e^{-i\mathbf{q} \cdot (\mathbf{r}-\mathbf{r}')} d^3r d^3r' \\ & = \frac{L_x L_y}{q_z^2} \exp \left[\frac{-q_z^2}{2} (\sigma_e^2 + \sigma_m^2) \right] \\ & \times \int \int \exp [q_z^2 C_{em}(X, Y) - i(q_x X + q_y Y)] dX dY, \end{aligned} \quad (5)$$

where L_x and L_y are the linear dimensions of the part of the sample probed by the beam.

Subtracting out the specular ($= \iint e^{-i(q_x X + q_y Y)} dX dY$) and combining everything, the difference signal in the diffuse scattering for a single system of scatterers is

$$\begin{aligned} \Delta \left(\frac{d\sigma}{d\Omega} \right)_{\text{diffuse}} = & P_c \frac{L_x L_y}{q_z^2} [\hat{k}_f \cdot \hat{m} + \cos(\alpha + \beta) \hat{k}_i \cdot \hat{m}] \exp \left[\frac{-q_z^2}{2} (\sigma_e^2 + \sigma_m^2) \right] \left[\left\{ N_e(-Zr_0) + N_r \frac{3\lambda}{8\pi} [F_1^1 + F_{-1}^1]^* \right\} \right. \\ & \left. \times N_r \frac{3\lambda}{8\pi} [F_{-1}^1 - F_1^1] + \text{c.c.} \right] \int \int \{ \exp [q_z^2 C_{em}(X, Y)] - 1 \} \exp [-i(q_x X + q_y Y)] dX dY. \end{aligned} \quad (6)$$

Finally, we extrapolate the above expression to a multilayer with N interfaces.¹³ With the simplifying assumption that the average positions of the charge interfaces correspond to those of the magnetic interfaces, the final result is

$$\begin{aligned}
\Delta \left(\frac{d\sigma}{d\Omega} \right)_{\text{diffuse}} &= P_c \frac{L_x L_y}{q_z^2} [\hat{k}_f \cdot \hat{m} + \cos(\alpha + \beta) \hat{k}_i \cdot \hat{m}] \sum_{i,j}^N \left[\Delta \rho_{em,ij} \exp \left[\frac{-q_z^2}{2} (\sigma_{e,i}^2 + \sigma_{m,j}^2) \right] \exp[iq_z(z_i - z_j)] \right. \\
&\times \int \int (\exp[q_z^2 C_{em,ij}(X,Y)] - 1) \exp[-i(q_x X + q_y Y)] dX dY + \Delta \rho_{em,ji}^* \exp \left[\frac{-q_z^2}{2} (\sigma_{e,j}^2 + \sigma_{m,i}^2) \right] \\
&\times \exp[iq_z(z_i - z_j)] \int \int (\exp[q_z^2 C_{em,ji}(X,Y)] - 1) \exp[-i(q_x X + q_y Y)] dX dY \left. \right], \quad (7)
\end{aligned}$$

where $\Delta \rho_{em,ij}$ is the difference across the i th interface of $\{N_e(-Zr_0) + N_r(3\lambda/8\pi)[F_1^1 + F_{-1}^1]^*\}$ times the difference across the j th interface of $\{N_r(3\lambda/8\pi)[F_{-1}^1 - F_1^1]\}$.

A couple of points should be noted about the expression in Eq. (7). The first is that the diffuse scattering difference signal scales with the value of P_c , and therefore an x-ray beam with a high degree of circular polarization is a necessity for efficient measurements. Second, interface roughness from magnetic moments oriented perpendicular to the scattering plane do not contribute to the diffuse scattering difference signal. And further, out-of-plane magnetic moments contribute negligibly since $\sin \alpha, \sin \beta \approx 0$. A final point that must be emphasized is that the technique of using circularly polarized photons to isolate the interference term probes charge-magnetic correlations and not pure magnetic correlations. A measurement of the latter type of correlation would require a different technique, such as magnetic scattering using the linearly polarized $\sigma \rightarrow \pi$ channel.

IV. FIT RESULTS

To fit the diffuse sum and difference data, layer thicknesses obtained from the specular reflectivity fit were fixed, and correlation functions appropriate for Gaussian roughness distributions were used. The form of the correlation function for both the charge and charge-magnetic fits is that for a self-affine fractal surface with a cutoff length, i.e., $C_{ee,i} = \sigma_{e,i}^2 \exp[-(R/\xi_{ee,i})^{2h_{ee,i}}]$ and $C_{em,i} = \sigma_{e,i} \sigma_{m,i} \exp[-(R/\xi_{em,i})^{2h_{em,i}}]$,¹² where ξ is the cutoff or correlation length and h is the Hurst parameter describing the texture of the roughness. For correlations between interfaces, the Schlomka *et al.*¹⁴ expression and its charge-magnetic analogue were used. Explicitly, they are:

$$\begin{aligned}
C_{ee,ij} &= \frac{\sigma_{e,i} \sigma_{e,j}}{2} \left\{ \exp[-(R/\xi_{ee,i})^{2h_{ee,i}}] \right. \\
&\quad \left. + \exp[-(R/\xi_{ee,j})^{2h_{ee,j}}] \right\} \exp[-|z_i - z_j|/\xi_{ee,\perp}], \\
C_{em,ij} &= \frac{\sigma_{e,i} \sigma_{m,j}}{2} \left\{ \exp[-(R/\xi_{em,i})^{2h_{em,i}}] \right. \\
&\quad \left. + \exp[-(R/\xi_{em,j})^{2h_{em,j}}] \right\} \exp[-|z_i - z_j|/\xi_{em,\perp}], \quad (8)
\end{aligned}$$

where $\xi_{ee,\perp}$ and $\xi_{em,\perp}$ are the out-of-plane correlation lengths for charge and charge-magnetic roughness correlations, respectively.

To fit the difference data, a magnetic moment profile within the Gd layers was required. This profile was obtained by fitting the difference offset data in Fig. 3 with the BA of Eq. (7). Each of the Gd layers was divided into three layers—two identical interfacial layers and a paramagnetic inner layer. The interfacial layers were assumed to be ferromagnetic, and the dipole transition matrix elements used in the fit were taken from Hamrick.¹⁵ An interfacial layer thickness of 7.8 Å was determined by the fit, which is shown in Fig. 3. In addition to determining the magnetic moment profile, the fit to the offset scan also provides information about the out-of-plane correlation length for charge-magnetic roughness (i.e., $\xi_{em,\perp}$). The value obtained through this fit was 670 Å, while a BA fit to the charge diffuse scattering—also shown in Fig. 3—resulted in a shorter out-of-plane correlation length for charge roughness of 440 Å.

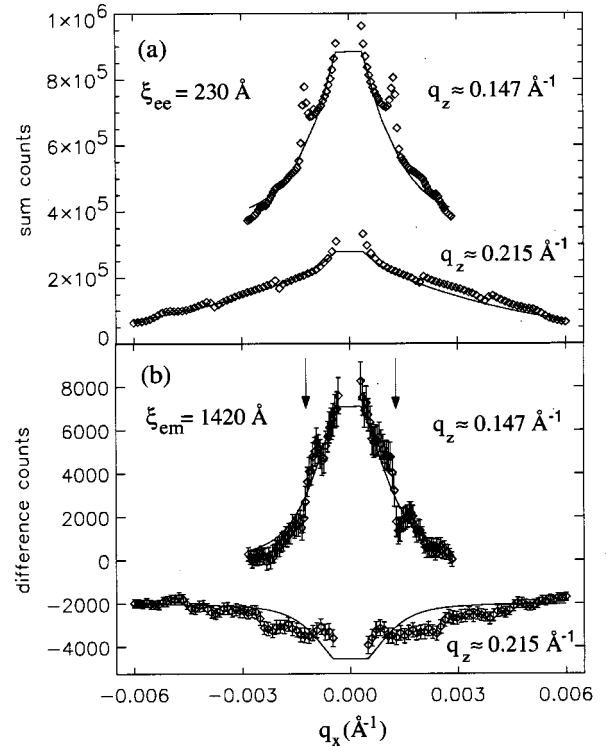


FIG. 4. BA fits (—) for (a) sum and (b) difference of opposite photon helicity rocking curve data (\diamond). Arrows indicate the anomalous scattering in the diffuse XRMS (see text). Statistical error bars for the summed data are smaller than the size of the symbol. Note that the data and fit at $q_z \approx 0.147 \text{ \AA}^{-1}$ have been shifted upward in (a) and the data and fit at $q_z \approx 0.215 \text{ \AA}^{-1}$ have been shifted downward in (b) for clarity.

In order to obtain the in-plane roughness correlation lengths, the BA for charge diffuse scattering and the BA of Eq. (7) were used to fit the two summed data and two difference data rocking curves, respectively. The magnetic moment distribution determined by the fit to the offset scan was used in the latter fit, and both fits are displayed in Fig. 4. From these fits, the correlation length for charge-magnetic roughness is again found to be longer than that for charge roughness (1420 Å with $h_{em}=0.71$ vs 230 Å with $h_{ee}=0.49$, respectively), in this case for the in-plane direction.

A striking feature of Fig. 4(b) that deserves comment is the structure in the data, indicated by arrows, which corresponds in reciprocal space to the anomalous scattering peaks in the summed data of Fig. 4(a). We believe this to be the first observation of such scattering in the diffuse XRMS. The peaks in Fig. 4(a) are due to the incident or exit angle satisfying the Bragg condition for the multilayer, and can be simulated by applying the distorted-wave Born approximation.^{12,16} The data of Figure 4(b) call for a similar treatment, and derivation of this theory is in progress.¹⁷

V. SUMMARY

A comparison of the fitted correlation lengths shows that the charge-magnetic roughness is “smaller” than the charge roughness in terms of having a longer in-plane correlation length. This is the same qualitative result seen by other groups,^{1,2,18} but the first such observation for a system with strong interfacial coupling. Through the use of hard x rays, which makes possible the study of out-of-plane roughness

correlations, the charge-magnetic roughness is also found to have a longer out-of-plane correlation length. While magnetic moments oriented in the out-of-plane direction could explain these observations, the demagnetizing fields that would result make this scenario unlikely.⁵ Other possible explanations include local variations in the Gd Curie temperature within the interfacial region and shape anisotropy, which favors a planar magnetic structure for the multilayer.

In conclusion, we have collected diffuse XRMS data from a multilayer that exhibits evidence of anomalous scattering and interference effects due to the different charge and magnetic structures of the multilayer. We have applied the BA to model the data and to obtain values for both the in-plane and out-of-plane correlation lengths for charge-magnetic roughness. By extracting this information from our fits, we have demonstrated that charge-magnetic roughness is smaller than charge roughness in a system with strong interfacial coupling and we have displayed the power that diffuse XRMS studies can bring to the important question of interface roughness.

ACKNOWLEDGMENTS

We thank Paul Reimer for use of his reflectivity and diffuse scattering fitting program and for helpful discussions. Work at the Advanced Photon Source was supported by the U.S. Department of Energy, Basic Energy Sciences, Office of Energy Research, under Contract No. W-31-109-ENG-38. H.H., N.I., and N.H. acknowledge support from Monbusho Grant-in-Aids for Scientific Research (No. 09236207 and No. 09305019).

¹J. F. Mackay, C. Teichert, D. E. Savage, and M. G. Lagally, *Phys. Rev. Lett.* **77**, 3925 (1996).

²J. W. Freeland, V. Chakarian, K. Bussmann, Y. U. Idzerda, H. Wende, and C.-C. Kao, *J. Appl. Phys.* **83**, 6290 (1998).

³L. G. Parratt, *Phys. Rev.* **95**, 359 (1954); L. Nevot and P. Croce, *Rev. Phys. Appl.* **15**, 761 (1980).

⁴E. E. Fullerton, J. E. Mattson, S. R. Lee, C. H. Sowers, Y. Y. Huang, G. Felcher, and S. D. Bader, *J. Magn. Magn. Mater.* **117**, L301 (1992); S. D. Bader (private communication).

⁵R. E. Camley and D. R. Tilley, *Phys. Rev. B* **37**, 3413 (1988).

⁶H. Hashizume, N. Ishimatsu, O. Sakata, T. Iizuka, N. Hosoito, K. Namikawa, T. Iwazumi, G. Srajer, C. T. Venkataraman, J. C. Lang, C. S. Nelson, and L. E. Berman, *Physica B* **248**, 133 (1998).

⁷N. Ishimatsu, H. Hashizume, S. Hamada, N. Hosoito, C. S. Nelson, C. T. Venkataraman, G. Srajer, and J. C. Lang, *Phys. Rev. B* **60**, 9596 (1999).

⁸R. E. Camley, *Phys. Rev. B* **39**, 12 316 (1989).

⁹R. M. Osgood III, S. K. Sinha, J. W. Freeland, Y. U. Idzerda, and S. D. Bader, *J. Magn. Magn. Mater.* **198-199**, 698 (1999).

¹⁰J. P. Hannon, G. T. Trammell, M. Blume, and D. Gibbs, *Phys. Rev. Lett.* **61**, 1245 (1988).

¹¹S. W. Lovesey and S. P. Collins, *X-Ray Scattering and Absorption by Magnetic Materials* (Oxford University Press, New York, 1996).

¹²S. K. Sinha, E. B. Sirota, S. Garoff, and H. B. Stanley, *Phys. Rev. B* **38**, 2297 (1988).

¹³S. K. Sinha, *J. Phys. III* **4**, 1543 (1994).

¹⁴J. P. Schlomka, M. Tolan, L. Schwalowsky, O. H. Seeck, J. Stettner, and W. Press, *Phys. Rev. B* **51**, 2311 (1995).

¹⁵M. D. Hamrick, M.A. thesis, Rice University, 1990.

¹⁶V. Holy, J. Kubena, I. Ohlidal, K. Lischka, and W. Plotz, *Phys. Rev. B* **47**, 15 896 (1993).

¹⁷S. K. Sinha (private communication).

¹⁸J. W. Cable, M. R. Khan, G. P. Felcher, and I. K. Schuller, *Phys. Rev. B* **34**, 1643 (1986).